Journal of Molecular Biomarkers & Diagnosis
ISSN: 2155-9929

Huang et al., J Mol Biomark Diagn 2016, 7:6
DOI: 10.4172/2155-9929.1000304

Research Article Open Access

Bis(Styryl) Terephthalonitrile-Derived Two-Photon Fluorescence Probe for Mercury Ions in Live Cells and Living Tissues

Chibao Huang[1]*, Guanglian Zhao[1], Xiaonan Liu[2], Daohai Zhang[3], Tingxiang Yuan[1] and Yang Liu[1]

[1]*Chemistry and Chemical Engineering College, Zunyi Normal University, Zunyi 563002, Guizhou, P. R. China*
[2]*The Hospital Infection Management Section, The Affiliated Baiyun Hospital of Guizhou Medical University, Guiyang, 550014, Guizhou, P. R. China*
[3]*Research and Development Department, National Engineering Research Center for Compounding and Modification of Polymeric Materials, Guiyang, 550014, Guizhou P. R. China*

Abstract

A novel two-photon fluorescence probe for Hg^{2+} derived from bis(styryl)terephthalonitrile as a two-photon fluorophore and bis [2-(2-hydroxyethyl sulfanyl) ethyl] amino group (ionophore) as a novel Hg^{2+} ligand was developed. The probe possesses small molecule size, large two-photon absorption cross-section (1067 GM) in H_2O, noncytotoxic effect, long-wavelength emission at 588 nm, large Stokes shift (121 nm), excellent photostability, high water-solubility, good cell-permeability, and pH-insensitivity in the biologically relevant range. The probe can selectively detect Hg^{2+} ions in live cells and living tissues without interference from other metal ions and the membrane-bound probes, and its quenching constant (K_{sv}^{TP}) is 8.73×10^5 M^{-1}.

Keywords: Bis(styryl)terephthalonitrile; Mercury; Cell-imaging; Two-photon fluorescence probe

Introduction

An insight of selective staining/imaging of specific cellular ions is of paramount importance for a deeper understanding of the character of each ion in a cellular system and their complex biological functions and processes [1-3]. Two-Photon (TP) excitation fluorescence microscopy (TPM), which uses two photons of lower energy as the excitation source, has rapidly evolved into a widely used tool in biological and biomedical research and is popular.

Ion-targeting two-photon excited fluorescence (TPEF) probes have increasingly drawn attention because of the laser light excitation of these probes, which offers number of advantages including deep tissue imaging, minimal photodamage to biological samples and bleaching to the probes, and low interference from the auto-fluorescence of a cell [4-6]. Various TPEF probes have been successfully designed and synthesized for lead ion [7], zinc ion [8-10], silver ion [11,12], glucose [13], cysteine/homocysteine [14], and thiols [15] in the past few years.

Mercury and its derivatives are widely used in industry, which causes adverse environment and health problems [16,17]. Concerns over toxic exposure to mercury provide motivation to explore new methods for monitoring aqueous Hg^{2+} in living cells. Either in plants or in animals, sensing of Hg^{2+} has been conducted by means of atomic absorption spectroscopy [18], X-ray microanalysis [19], or $^{203}Hg^{2+}$ detection which usually needs expensive apparatus and/or sample preparation and pays the price of damaging the living organisms [20]. However, fluorescent chemodosimeters provide a promising way for simple and rapid tracking of Hg^{2+} in biological systems. But, only a few of these fluorescent probes have been utilized successfully in living cells [21], as fluorescent chemodosimeters for Hg^{2+} detection are often limited by nonspecific interference from Cu^{2+} and other competing metal ions [22,23], or are incompatible with aqueous media and living cells [24], and/or delay Hg^{2+} response [25].

Although many one-photon sensors for mercury ion have been developed [26-29], only a few two-photon fluorescence chemodosimeter for mercury ion were reported [30-32]. But, one among these three probes is used just for bioimaging and has a considerably small δ value. Thus it can be seen that the development of two-photon fluorescence sensors for mercury ion is not only indispensable to biological chemistry but also really challenging.

Recently, we reported a mercury TPEF probe for Hg^{2+} derived from 4-methyl-2,5-dicyano-4'-amino stilbene (DCS) as a TP fluorophore and bis[2-(2-hydroxyethyl sulfanyl)ethyl]amino group (HSA) as a novel Hg^{2+} ligand [33]. Although this probe exhibited excellent selectivity for Hg^{2+}, it was not applied to live cell and living Tissues imaging.

Herein, we extend our earlier work [33] and report a new TPEF probe for Hg^{2+} derived from bis(styryl) terephthalonitrile as a two-photon fluorophore and bis[2-(2-hydroxyethyl sulfanyl) ethyl]amino group (ionophore) as a novel Hg^{2+} ligand, which contains two sulfur atoms known as "soft base" capable of chelating so called "soft acid" heavy metal cations, and exhibits a good affinity to Hg^{2+}. We report that BHg (Figure 1) is capable of imaging Hg^{2+} ions in live cells without mistargeting and photobleaching problems.

Experimental

Materials and Methods

NMR spectra were recorded on a VARIAN INOVA 400 MHz NMR spectrometer. Mass spectral determinations were made on a ESI-Q-TOF mass spectrometry (Micromass, UK). High resolution mass spectra measurements were performed on a GC-TOF mass spectrometry (Micromass, UK). Fluorescence measurements were performed on a PTI-C-700 felix and time-master system. Fluorescence quantum yields were measured using standard methods [34] on air-equilibrated samples at room temperature. Quinine bisulfate in 0.05

***Corresponding author:** Chibao Huang, Chemistry and Chemical Engineering College, Zunyi Normal University, Zunyi 563002, Guizhou, P. R. China, Tel: 0086-852-8927159; E-mail: huangchibao@163.com

Received July 05, 2016; **Accepted** August 28, 2016; **Published** August 31, 2016

Citation: Huang C, Zhao G, Liu X, Zhang D, Yuan T, et al. (2016) Bis(Styryl) Terephthalonitrile-Derived Two-Photon Fluorescence Probe for Mercury Ions in Live Cells and Living Tissues. J Mol Biomark Diagn 7: 303. doi: 10.4172/2155-9929.1000303

Copyright: © 2016 Huang C, et al. This is an open-access article distributed under the terms of the Creative Commons Attribution License, which permits unrestricted use, distribution, and reproduction in any medium, provided the original author and source are credited.

mol L^{-1} H_2SO_4 (Φ=0.546) was used as a reference [34]. TPEF (two-photon-excited fluorescence) action cross-section spectra were measured according to the experimental protocol established by Xu and Webb [35], using a mode-locked Ti/sapphire laser that delivers ~80 fs pulses at 76 MHz. Fluorescein (10^{-4} mol L^{-1} in 0.1 mol L^{-1} NaOH), whose TPEF action cross-sections are well-known [35], served as the reference. The quadratic dependence of the fluorescence intensity on the excitation intensity was verified for each data point, indicating that the measurements were carried out in intensity regimes in which saturation or photodegradation does not occur. The measurements were performed at room temperature on air-equilibrated solutions (10^{-5} mol L^{-1}). The experimental uncertainty on the absolute action cross-sections determined by this method has been estimated to be ± 20% [35]. Absorption spectra were measured on a HP-8453 spectrophotometer. Solvents were generally dried and distilled prior to use. Reactions were monitored by thin-layer chromatography on Merck silica gel 60 F_{254} pre-coated aluminum sheets. Column chromatography: Merck silica gel Si 60 (40 μm to 63 μm, 230-400 mesh). The pH-dependent fluorescence studies were performed according to the literature [36].

Synthesis

2,5-bis((E)-4-(bis(2-chloroethyl) amino) styryl) terephthalonitrile (8): Aldehyde 2 (560 mg, 2.28 mmol), and NaH (55 mg, 2.28 mmol) were dissolved in 3 mL of tetrahydrofuran (THF), and the solution was cooled to 0°C under N_2. To this solution, phosphonate 7 (488 mg, 1.14 mmol) in 9 mL of THF was added dropwise. The reaction mixture was stirred for 1 h at 0°C, and then for 12 h at room temperature, followed by the removal of THF under reduced pressure. Water was added to the reaction mixture, and the product was extracted with dichloromethane (4 × 10 mL). The organic layer was dried with dry Na_2SO_4 followed by evaporation of the solvent. The crude product was separated by column chromatography with a gradient of hexane in dichloromethane (20% to 0%) and ethyl acetate in dichloromethane (0% to 20%). The resulting solid was recrystallized from acetone to give compound 8 (453 mg, 65%) as a yellow powder.

IR (KBr) cm^{-1}: 2223 (C≡N) and 1594~1348 (C=C).

HRMS (EI) m/z: 610.1225 (calcd for $C_{32}H_{30}C_{l4}N_4$: 610.1225).

^{1}H NMR (DMSO-d^6, 400 MHz) ppm: 8.446 (s, 2H, Ph), 7.620 (d, 2H, J=16.4 Hz, CH=CH), 7.498 (d, 4H, J=8.4 Hz, Ph), 7.054 (d, 2H, J=16.4 Hz, CH=CH), 6.844 (d, 4H, J=8.8 Hz, Ph), 3.772 (t, 8H, J_1=J_2=4.4 Hz, NCH_2), 3.712 (t, 8H, J_1=J_2=2 Hz, CH_2Cl)

Elemental analysis: calculated for $C_{32}H_{30}C_{l4}N_4$ (MW 612.42) C 62.76, H 4.94, Cl 23.16, N 9.15%; Found C 62.80, H, 4.98, Cl 23.13, N 9.10%.

2,5-bis((E)-4-(bis(2-(2-hydroxyethylthio) ethyl) amino) styryl) terephthalonitrile (BHg): Compound 8 (306 mg, 0.5 mmol), 2-mercaptoethanol (172 mg, 2.2 mmol), and anhydrous K_2CO_3 (414 mg, 3 mmol) were dissolved in acetone (25 mL), then the mixture was refluxed for 24 h with stirring under N_2. The resulting mixture was filtered, and the filtrate was concentrated by evaporating the solvent to get a viscous liquid. The crude product was purified by column chromatography using acetone/dichloromethane to afford compound BHg (335 mg, 86%) as a red solid. Further purification could be achieved by recrystallization from methanol to give needle solid.

IR (KBr) cm^{-1}: 3422 (OH), 2922 (CH), 2220 (C≡N) and 1631~1349 (C=C).

HRMS (EI) m/z: 778.2715 (calcd for $C_{40}H_{50}N_4O_4S_4$: 778.2715).

^{1}H NMR ($CHCl_3$-d, 400 MHz) ppm: 8.442 (s, 2H, Ph), 7.620 (d, 2H, J=16.0 Hz, CH=CH), 7.513 (d, 4H, J=8.8 Hz, Ph), 7.055 (d, 2H, J=16.0 Hz, CH=CH), 6.789 (d, 4H, J=8.4 Hz, Ph), 4.918 (t, 8H, J=4.8 Hz, 4 × OCH2), 3.633 (t, 8H, J_1=J_2=6.0 Hz, 4 × NCH_2), 2.791 (t, 8H, J_1=6.8 Hz, J_2=7.6 Hz, 4 × SCH_2), 2.728 (t, 8H, J1=6.8 Hz, J_2=6.4 Hz, 4 × SCH_2), 2.564 (s, 4H, 4 × OH). ^{13}C NMR (CHC_{l3}-d, 100 MHz) ppm: 147.68, 138.02, 134.96, 129.36, 128.88, 123.48, 117.03, 116.12, 113.15, 111.64, 61.23, 50.69, 34.11, 28.69.

Elemental analysis: calculated for $C_{40}H_{50}N_4O_4S_4$ (MW 779.11) C 61.66, H 6.47, N 7.19, O 8.21, S 16.46%; Found C 61.71, H 6.54, N 7.16, O 8.17, S 16.42%.

Results and discussion

Design and synthesis of 2,5-bis((E)-4-(bis(2-(2-hydroxyethylthio) ethyl) amino) story) terephthalonitrile (BHg)

2,5-dibromo-p-xylene (4) [37], 2,5-dimethyl-terephthalonitrile (5) [37], 2,5-bis(bromomethyl)terephthalonitrile (6) [37],1,4-Bis(diethylphosphorylmethyl)-2,5-dicyanob-benzene (7) [38] and 4-[Bis(2-chloro-ethyl) amino] benzaldehyde (2) [39] were synthesized according to literature procedures. The nucleophilic substitution of 8 and 2-mercaptoethanol gave BHg in high yield (86%) (Scheme 1). In the reaction of 8 and 2-mercaptoethanol, the substitution of no hydroxy group but mercapto group for chloro group was observed, because the nucleophilic strength of mercapto group is superior to that of hydroxy group.

Selectivities of Sensor BHg for Metal Ions

The solubility of BHg in water was 576 μM, which is sufficient to stain the cells (Supplementary Figure S1), Supporting Information (SI)). To obtain insight into the binding properties of BHg toward metal ions, the fluorescent spectrum changes were investigated upon addition of various metal ions (Ag^+, Ca^{2+}, Cd^{2+}, Cr^{3+}, Fe^{3+}, Co^{2+}, Ni^{2+}, Fe^{2+}, Na^+, Cu^{2+}, Zn^{2+}, Mn^{2+}, Mg^{2+}, Hg^{2+}, Pb^{2+}, K^+, and Ba^{2+}) to 30 mM MOPS buffer (100 mM KCl, 10 mM EGTA, pH 7.2. EGTA=ethylene glycol bis(2-aminoethyl ether) N,N,N',N'-tetraacetic acid, and MOPS=3-(morpholino) propanesulfonic acid) of BHg (Figure 2), respectively. The experimental results suggest that BHg shows a notable selectivity to Hg^{2+}. As depicted in Figure 2, BHg displays scarcely any response to other metal ions and weak complexation with Ag^+, Pb^{2+} and Cu^{2+}. The highly selective recognition of BHg for mercury ion can be attributed to two factors. On the one hand, a sulfur atom and Hg^{2+} are typical "soft base" and "soft acid", respectively; and the very strong affinity between them is quite natural. On the other hand, the nitrogen atom properties and the numbers of sulfur atoms in open chain monoazadithiacrown ether may play an important role in the affinities of nitrogen and sulfur atoms to heavy-metal-ion.

Sensitivity of sensor BHg to Hg^{2+} in UV-Vis, one- and two-photon excited fluorescence spectra

Notably, upon complexation with Hg^{2+}, two characteristic strong

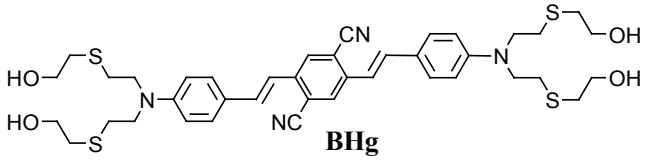

Figure 1: Molecular structure of probe BHg.

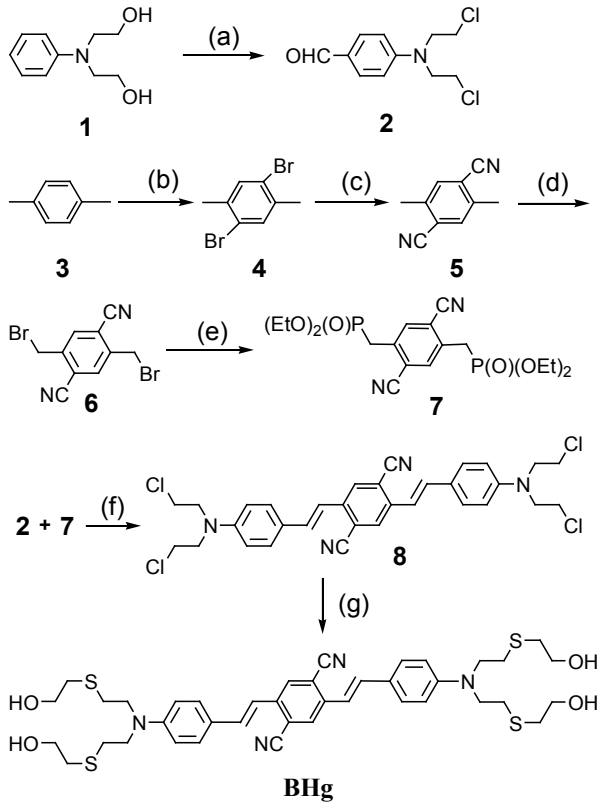

Scheme 1: Synthetic procedures of compound BHg (reagent and conditions: (a) $POCl_3$/DMF, 90°C, 2 h (95%); (b) Br_2/CH_2Cl_2, no light, 20°C, 24 h (90%); (c) CuCN/DMF, 150°C, 48 h (78%); (d) NBS/CCl_4, 6 h (15%); (e) $P(OEt)_3$/toluene, 120°C, 5 h (96%); (f) NaH (2 equiv)/THF, 12 h (65%); (g) K_2CO_3/MeCN, $HS(CH_2)_2OH$, 40°C, 12 h (86%).

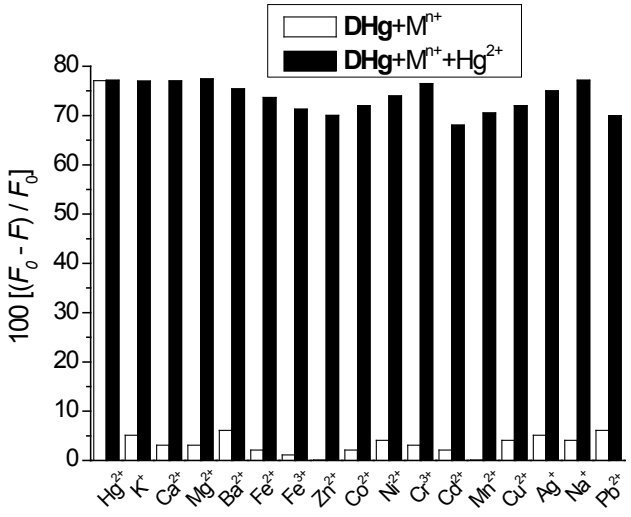

Figure 2: A comparison of the percent quenching of one-photon excited fluorescence of BHg (1 μM) at 588 nm in the presence of 20 mM for Zn^{2+}, K^+, Ca^{2+}, Mg^{2+}, Ba^{2+}, Fe^{2+}, Fe^{3+}, Pb^{2+}, Co^{2+}, Ni^{2+}, Cr^{3+}, Cd^{2+}, Mn^{2+}, Cu^{2+}, Ag^+, Na^+ and Pb^{2+} (empty bars) followed by addition of 40 μM of Hg^{2+} (filled bars). These data were measured in 30 mM MOPS buffer (100 mM KCl, 10 mM EGTA, pH 7.2).

absorption bands of BHg transferred from 467 and 269 nm to 426 and 284 nm, respectively, a hypochromatic shift of 41 nm and a bathochromic shift of 15 nm occurred with the cation-binding event, and the absorption band centered at 467 nm and the absorption band centered at 269 nm declined and enhanced gradually, respectively (Figure 3). The quenching constant (KsvAb) of BHg for mercury ion was determined from the absorption-titration curves to be 8.24 × 105 M^{-1} and 4.36 × 104 M^{-1} at 20°C in 30 mM MOPS buffer (Supplementary Figures S1 and S2).

BHg exhibits a very strong sensitivity to Hg^{2+} in the OP and TP processes (Figures 4 and 5), and the emission band of BHg centered at 587 nm progressively decreased upon the addition of Hg^{2+} to the solution. The quenching of BHg shows a downward non-linear curvature in the Stern-Volmer plot (I587 *vs* [Hg^{2+}]) in a broader Hg^{2+} concentration (0 μM to 40 μM) (Supplementary Figures S3-S5) range. The quenching constants (K_{sv}OP and K_{sv}TP) for BHg calculated from the OP and TP fluorescence titration curves (Figures 4 and 5) are 5.25 × 105 M^{-1} (2.76 × 104 M^{-1}) and 6.94 × 105 M^{-1} (2.24 × 104 M^{-1}) (Supplementary Figures S1,S3 and S5), respectively; the detection limit of the probe is in the micromolar range. However, in a narrower concentration (0.10 μM to 10 μM) range, two linear Stern-Volmer plots are obtained with Stern-Volmer constants of K_{sv}OP=8.59 × 105 M^{-1} and K_{sv}TP = 8.73 × 105 M^{-1} (Supplementary Figures S1, S4 and S6). BHg is strongly fluorescent in CH_2C_{l2} (Φ=0.83) and H_2O (Φ=0.62). This means that BHg can serve as a good sensor for mercury ion applied to OPF and TPF detection.

Job's plot for BHg-Hg^{2+} complex

For the complexation ratio between the ligand and the metal ion,

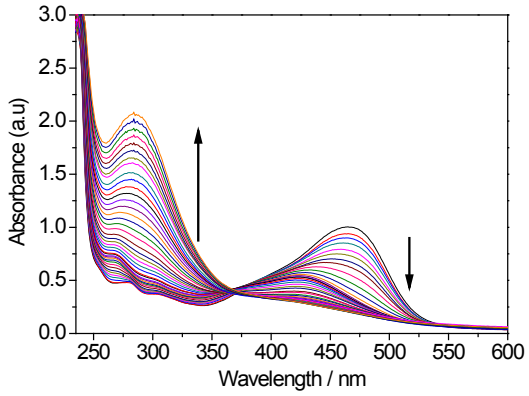

Figure 3: The absorption spectra of BHg (10 μM) in 30 mM MOPS buffer (100 mM KCl, 10 mM EGTA, pH 7.2) after addition of Hg^{2+} (0 μM to 40 μM).

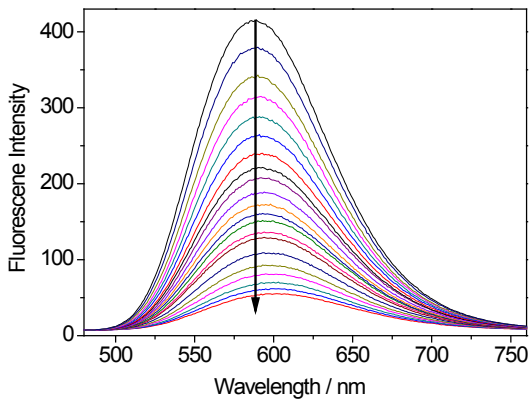

Figure 4: OP emission spectra of BHg (1.0 μM) in 30 mM MOPS buffer (100 mM KCl, 10 mM EGTA, pH 7.2) after addition of Hg^{2+} (0 μM to 40 μM).

a Job plot experiment was conducted by varying the concentration of both BHg and Hg^{2+}. Solutions of BHg and Hg^{2+} in 30 mM MOPS buffer in different mole fractions were prepared by mixing BHg and Hg^{2+} in H_2O in appropriate ratios while maintaining the total concentration to 1.0 μmol L^{-1}. The absorbance of each solution at 467 nm was measured. The concentration of BHg-Hg^{2+} complex for each solution was calculated by using the UV absorption data and the quenching constant (Supplementary Figure S4). The plot of (complex) vs the mole fraction of Hg^{2+} shows a maximum when the mole fraction is 0.67, indicating that BHg is coordinated with Hg^{2+} with 1:2 stoichiometry in water solution (Supplementary Figure S7-S13).

Two-photon absorption cross section of BHg versus two-photon excited wavelength

δ of BHg was determined by using the two-photon-induced fluorescence measurement technique [35]. As expected, δ of BHg decreased 2.7-fold from 1067 to 294 GM upon the addition of 20 μM Hg^{2+} to the solution (Figure 6). TP excitation of BHg produced similar emission spectra compared to OP excitation. Likewise, its two-photon excitation spectra are analogous to the OP absorption spectra, and it had a TP excitation maximum at 810 nm. When excess Hg^{2+} was added, δ decreased even further, probably because the electron-donating ability of the aromatic amino moiety is attenuated upon complexation.

One-Photon Fluorescence Spectra of Sensor BHg versus pH

The fluorescence of BHg was also slightly weakened by protonation of the tertiary amine in the bis(styryl)terephthalonitrile skeleton upon pH <4.5 or so, and remained unchanged at pH 4.5-13 (Figure 7). The enhancement of the fluorescence at high pH and quenching by H^+ and Hg^{2+} are consistent with a ICT mechanism from the aromatic amines. Therefore, BHg is pH-insensitive in the biologically relevant pH range.

Two-photon Scanning Microscopy Imaging

For two-photon *in vitro* imaging, cells were imaged in the tissue culture chamber (5% CO_2, 37°C) using a Zeiss 510 LSM (upright configuration) confocal microscope equipped with a femtosecond-pulsed Ti:sapphire laser (Mira 900-F, Coherent). The excitation beam produced by the femtosecond laser, which was tunable from 700 nm to 1100 nm (λ_{ex}=810 nm, ~1.5 W), passed through an LSM 510 microscope with HFT 650 dichroic (Carl Zeiss, Inc.) and focused onto the coverslip-adherent cells using a 63× oil immersion objective (NA 1.4). The NLO META scan head allowed data collection in 10.7 nm windows at 610 nm, and a bypass filter of 550 nm to 650 nm was used for collection of the emission light.

Details of the preparation of the mouse fibroblast culture are given in the SI. The TPM images of mouse fibroblast labeled with BHg showed very strong TPF at 550 nm to 650 nm (Figure 8a), and the high contrast and good resolution were observed, indicating BHg has a considerably desired cell-imaging effect and good cell-permeability. After addition of 20 μM Hg^{2+} to the imaging solution and the incubation at 37°C under 5% CO_2 for 15 min, the TPF intensity decreased rapidly, and the TPM image became shaded and obscure (Figure 8b). Without interference from the membrane-bound probes (due to no fluorescence at 360 nm to 460 nm) in this visual window, therefore, BHg can detect Hg^{2+} concentrations in live cells and has noncytotoxic effect.

To further investigate the utility of this probe in deep tissue imaging, TPM images were obtained from a part of a mouse brain tissue slice incubated with 10.0 μM BHg for 30 min at 37°C. Two TPM images were obtained in the same plane at a depth of about 120 μm. Without the addition of Hg^{2+}, the TPM image was bright (Figure 9a), while, after the addition of Hg^{2+}, the emission was clearly diminished (Figure 9b). This result demonstrate that BHg is capable of detecting intracellular Hg^{2+} ions at a depth of 120 μm in living tissues by using TPM.

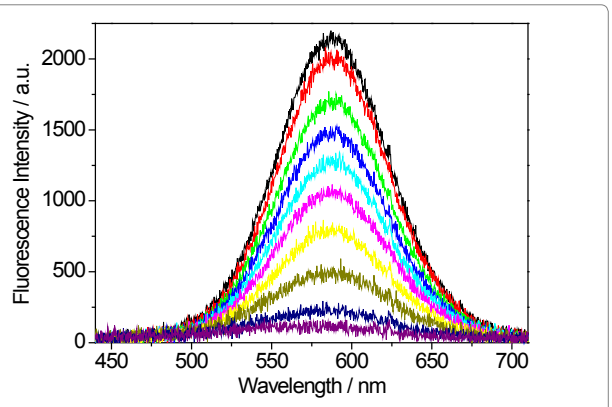

Figure 5: TP emission spectra of BHg (1.0 μM) in 30 mM MOPS buffer (100 mM KCl, 10 mM EGTA, pH 7.2) after addition of Hg^{2+} (0 μM to 40 μM).

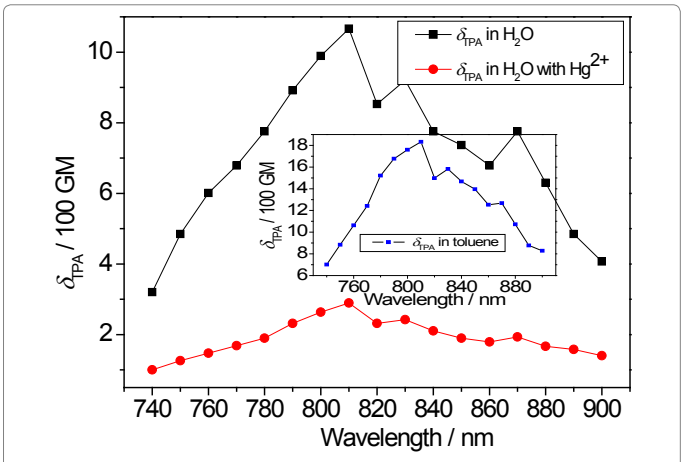

Figure 6: Two-photon excitation spectra of BHg (1.0 μM) before (■) and after (△) addition of 20 equiv of Hg^{2+} in 30 mM MOPS buffer (100 mM KCl, 10 mM EGTA, pH 7.2).

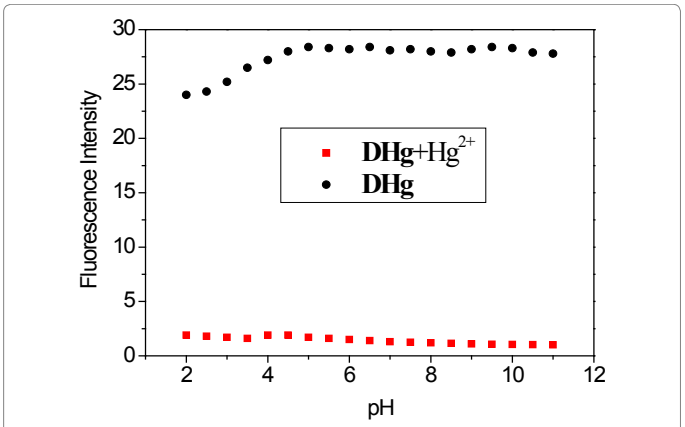

Figure 7: Effect of the pH on the one-photon fluorescence intensity of 1.0 μM BHg in the presence of 0.0 (●) and 1.0 μM (■) of free Hg^{2+}. pH was adjusted with HCl, NaCl and NaOH. The excitation wavelength was 467 nm.

Building a calibration curve for a Hg^{2+}-BHg complex

All reagents were of the highest purity available and at least of analytical reagent grade. The standard stock solution of lead (Ⅱ) was prepared by dissolving the appropriate amount of mercury nitrate and a small amount of HNO_3 in double distilled water. A series of standard solutions of Hg^{2+} may be prepared with different concentrations by appropriate dilution of the stock solution with water, and are calibrated by volumetric analysis. As seen in (Figure S6) (SI), the TPF intensities of BHg (1.0 μM) show a linear correlation of Hg^{2+} concentrations from 1.0×10^{-7} to 1.6×10^{-5} mol L^{-1}. The TPF intensities are plotted versus the solution standard concentrations, and the points should form a straight line. This line, called a calibration curve, shows how changes in TPF intensity with the concentration of a solution.

A calibration curve of the TPF intensities for BHg (1.0 μM) versus the Hg^{2+} concentrations from 1.0×10^{-7} to 1.6×10^{-5} mol L^{-1} was obtained by fitting a linear equation to the data in Table 1. The calibration curve is equivalent to the equation 1 (Figure 10). In Figure 10, the correlation coefficient (r) and the population correlation coefficient (ρ) are r = -0.99888 and p<0.0001, respectively. This indicates that there is a good linear correlation between the TPF intensities and the Hg^{2+} concentrations from 1.0×10^{-7} to 1.6×10^{-5} mol L^{-1}.

$$Y = -2407.07 - 13536.52 \times \log [Hg^{2+}] \quad (1)$$

Conclusion

In conclusion, we have developed a TPF probe BHg with small molecule size, large TP absorption cross-section (1067 GM), noncytotoxic effect, long-wavelength emission at 587 nm (adjacent to the ideal imaging visual window 650 nm to 900 nm), large Stokes shift (120 nm), excellent photostability, moderate water-solubility and good cell-permeability. BHg is pH-insensitive in the biologically relevant range, and its quenching constant (K_{sv}TP) is 8.73 × 105 M^{-1}. This novel probe can selectively detect Hg^{2+} ions in live cells and living tissues at a depth of 120 μm without interference from other metal ions and the membrane-bound probes.

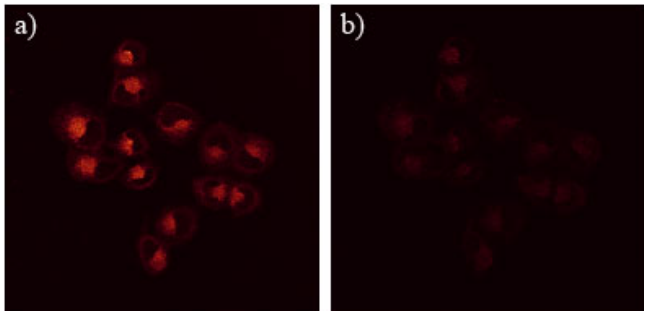

Figure 8: TPM images of 1.0 μM BHg-labelled mouse fibroblast collected at 550 nm to 650 nm, before (a) and after (b) addition of 20 μM Hg^{2+} to the imaging solution. The two-photon excitation fluorescence (TPEF) images were collected upon excitation at 810 nm with a femtosecond pulse. Cells shown are representative images from replicate experiments (n=5).

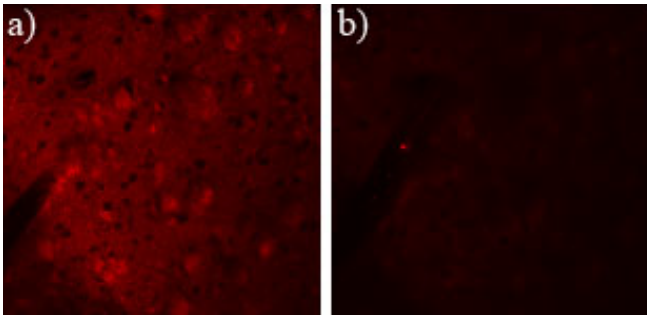

Figure 9: TPM images of a mouse brain tissue slice stained with 10.0 μM BHg at a depth of ca. 120 μm with magnification 100×. Before (a) and after (b) addition of 20.0 μM Hg^{2+} to the imaging solution. The two-photon excitation fluorescence (TPEF) images were collected at 550 nm to 650 nm upon excitation at 810 nm with a femtosecond pulse. Cells shown are representative images from replicate experiments (*n*=5).

Serial number	X [a]	Y [b]
1	1.00E-07	720
2	1.50E-07	680.32
3	2.00E-07	635.12
4	3.00E-07	601.89
5	4.00E-07	550.38
6	6.00E-07	511.45
7	7.00E-07	496.51
8	1.00E-06	438.21
9	1.50E-06	386.54
10	2.00E-06	340.09
11	2.50E-06	298.47
12	3.50E-06	257.78
13	4.50E-06	217.28
14	5.50E-06	185.98
15	7.50E-06	155.46
16	1.00E-05	125.75
17	1.25 E-05	100.00
18	1.40 E-05	70.00
19	1.60 E-05	40.00

[a] (Hg^{2+}) / mol L^{-1} ; [b] Relative TPF Intensity

Table 1: Relative TPF intensities of BHg (1.0 μM) at 587 nm under different Hg^{2+} concentrations.

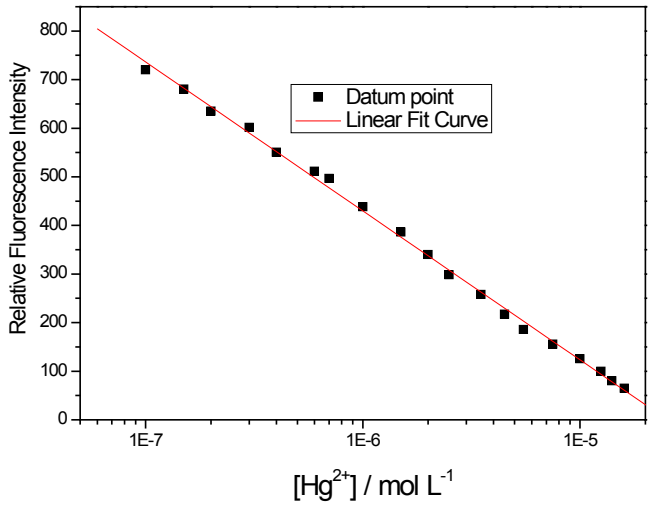

Figure 10: The calibration curve of the TPF intensities for BHg (1.0 μM) at 587 nm versus the Hg^{2+} concentrations from 1.0×10^{-7} to 1.6×10^{-5} mol L^{-1}.

Acknowledgments

Financial supports from the National Natural Science Foundation of China (Nos. 21562050), the Special Fund Project of the construction of the Eighth Batch of Scientific and Technological Innovation Talent Team in Guizhou Province [No. (2015)4007], Guizhou science and technology fund project (Nos. J[2015]2146, J LKZS [2012]23, J LKZS [2012]13), the Key Project of Education Department of

Guizhou Province (Nos. KY[2014]296), KY(2013)171), Teaching Contents and Curriculum System Reform Project of Higher Education in Guizhou Province (No. KY [2014] JXGChcb), Project of "15851 Talents Elite Project" in Zunyi City ((2015)4007) and the Science and Technology Project of Zunyi city Honghuagang District (No. [2015]18) are deeply acknowledged.

References

1. Kim HM, Jung C, Kim BR, Jung SY, Hong JH, et al. (2007) A two-photon fluorescent probe for lipid raft imaging: C-laurdan. Chem Int Ed 46: 3460-3463.
2. Kim HM, Kim BR, Hong JH, Park JS, Lee K J, et al. (2007) A two-photon fluorescent probe for calcium waves in living tissue. Chem Int Ed 46: 7445-7448.
3. Kim MK, Lim CS, Hong JT, Han JH, Jang HY, et al. (2010) High-fidelity hydrophilic probe for two-photon fluorescence lysosomal imaging. Chem Int Ed 49: 364-367.
4. Masters BR, Peter TC (2006) Confocal microscopy and multiphoton excitation microscopy: the genesis of live cell imaging. SPIE.
5. So PT, Dong CY, Masters BR, Berland KM (2000) Two-photon excitation fluorescence microscopy. Annu Rev Biomed Eng 2: 399-429.
6. Guo L, Wong MS (2014) Multiphoton excited fluorescent materials for frequency upconversion emission and fluorescent probes. Adv Mater 26: 5400-5428.
7. C. Huang, C. Ding,(2011) Dicyanostilbene-derived two-photon fluorescence probe for mercury ions in live cells and living tissues. Analytica Chimica Acta 699 (2): 198-205
8. Huang C, Qu J, Qi J, Yan M, Xu G (2011) Dicyanostilbene-derived two-photon fluorescence probe for free zinc ions in live cells and tissues with a large two-photon action cross section. Org Lett 13: 1462-1465
9. Sumalekshmy S, Henary MM, Siegel N, Lawson PV, Wu Y, et al. (2007) Design of emission ratiometric metal-ion sensors with enhanced two-photon cross section and brightness. J Am Chem Soc 129: 11888-11889.
10. Kim HM, Seo MS, An MJ, Hong JH, Tian YS, et al. (2008) Two-Photon Fluorescent Probes for Intracellular Free Zinc Ions in Living Tissue. Chem Int Ed 47: 5167-5170.
11. Huang C, Ren A, Feng C, Yang N (2010) Two-photon fluorescent probe for silver ion derived from twin-cyano stilbene with large two-photon absorption cross section. Sensors and Actuators B: Chemical 151: 236-242.
12. Huang C, Peng X, Lin Z, Fan J, Ren A, et al. (2008) A highly selective and sensitive two-photon chemosensor for silver ion derived from 3,9-dithia-6-azaundecane, Sensors and Actuators B: Chemical.133: 113-117.
13. Tian YS, Lee HY, Lim CS, Park J, Kim HM, et al. (2009) A two-photon tracer for glucose uptake. Chem Int Ed.48: 8027-8031.
14. Zhang M, Yu M, Li F, Zhu M, Li M, et al. (2007) A highly selective fluorescence turn-on sensor for cysteine/homocysteine and its application in bioimaging. J Am Chem Soc 129: 10322-10323.
15. Lee JH, Lim CS, Tian YS, Han J H, Cho BR (2010) A two-photon fluorescent probe for thiols in live cells and tissues. J Am Chem Soc132: 1216-1217.
16. Harris HH, Pickering IJ, George GN (2003) The chemical form of mercury in fish. Science 301: 1203.
17. Harada M (1995) Minamata disease: methylmercury poisoning in Japan caused by environmental pollution. Crit Rev Toxicol 25: 1.
18. Palmeira CM, Moreno AJ, Madeira VM (1994) Interactions of herbicides 2,4-D and dinoseb with liver mitochondrial bioenergetics. Toxicol Appl Pharmacol 127: 50.
19. Endo T, Sakata M, Shaikh ZA (1995) Mercury uptake by primary cultures of rat renal cortical epithelial cells: 1. effects of cell density, temperature, and metabolic-inhibitors. Toxicol Appl Pharmacol 132: 36.
20. Bridges CC, Zalups RK (2004) Molecular and ionic mimicry and the transport of toxic metals. Am J Pathol 165: 1385.
21. Zhang Z, Wu D, Guo X, Qian X, Lu Z, et al. (2005) Visible study of mercuric ion and its conjugate in living cells of mammals and plants. Chem Res Toxicol 18: 1814.
22. Xu Z, Qian X, Cui J (2005) Colorimetric and ratiometric fluorescent chemosensor with a large red-shift in emission: Cu(II)-only sensing by deprotonation of secondary amines as receptor conjugated to naphthalimide fluorophore. Org Lett 7: 3029.
23. Martınez R, Espinosa A, Tarraga A, Molina P (2005) New Hg^{2+} and Cu^{2+} selective chromo- and fluoroionophore based on a bichromophoric Azine. Org Lett 7: 5869.
24. Prodi L, Bargossi C, Montalti M, Zaccheroni N, Su N, et al. (2000) An effective fluorescent chemosensor for mercury ions. J Am Chem Soc 122: 6769.
25. Rurack K, Kollmannsberger M, Resch-Genger U, Daub J (2000) A selective and sensitive fluoroionophore for hgii, agi, and cuii with virtually decoupled fluorophore and receptor units. J Am Chem. Soc 122: 968.
26. Ono A, Togashi H (2004) Möbius Aromatic Hydrocarbons: Challenges for Theory and Synthesis. Angew Chem 116: 4396-4400.
27. Zheng H, Qian ZH, Xu L, Yuan FF, Lan LD, et al. (2006) Switching the recognition preference of rhodamine b spirolactam by replacing one atom: Design of Rhodamine B Thiohydrazide for recognition of Hg(II) in aqueous solution Org. Lett 8: 859-861.
28. Nolan EM, Lippard SJ (2003) A “turn-on” fluorescent sensor for the selective detection of mercuric ion in aqueous media. J Am Chem Soc 125: 14270-14271.
29. Dai H, Liu F, Gao Q, Fu T, Kou X (2011) A highly selective fluorescent sensor for mercury ion (II) based on azathia-crown ether possessing a dansyl moiety. Luminescence, 26 : 523-530
30. Wu Y, Dong Y, Li J, Huang X, Cheng Y, et al. (2011) A Highly Selective and Sensitive Polymer-ased Fluorescence Sensor for Hg2+-Ion Detection via Click Reaction. Chem Asian J 6: 2725-2729
31. Lim CS, Kang DW, Tian YS, Han JH, Hwang HL, et al. (2010) Detection of mercury in fish organs with a two-photon fluorescent probe. Chem Commun 46: 2388-2390
32. Bell J, Samb I, Toullec PY, Mongin O, Blanchard-Desce M, et al. (2014) Ultra-sensitive and selective Hg^{2+} chemosensors derived from substituted 8-hydroxyquinoline analogues. New J Chem 38: 1072-1078
33. Huang C, Fan J, Peng X, Lin Z, Guo, et al. (2008) Highly selective and sensitive twin-cyano-stilbene-based two-photon fluorescent probe for mercury (ii) in aqueous solution with large two-photon absorption cross-section. J Photochem Photobio A: Chem 199 (2-3): 144-149.
34. Eaton DF (1988) Reference materials for fluorescence measurement. J photochem Photobiol Bbiol 2: 523-531.
35. Xu C, Webb WW (1996) Measurement of two-photon excitation cross sections of molecular fluorophores with data from 690 to 1050 nm. J Opt Soc Am B 13: 481-491.
36. Burdette SC, Walkup GK, Spingler B, Tsien RY, Lippard SY (2001) Fluorescent Sensors for Zn^{2+} Based on a Fluorescein Platform: Synthesis, Properties and Intracellular Distribution. J Am Chem Soc 123: 7831-7841.
37. Huang H, He Q, Lin H, Bai F, Sun Z, et al. (2004) Synthesis and photophysical properties of a novel semiconducting polymer. Polym Adv Technol 15: 84-88.
38. Wenseleers W, Stellacci F, Meyer-Friedrichsen T, Mangel T, Bauer CA, et al. (2002) Five Orders-of-Magnitude Enhancement of Two-Photon Absorption for Dyes on Silver Nanoparticle Fractal Clusters. J Phys Chem B 106: 6853-6863.
39. Wiley RH, Irick G (1961) Notes. 4[N, N-Bis(2-haloethyl) amino]benzaldehyde Derivatives. J Org Chem 26: 593-595.